

---

# Task-Agnostic Online Reinforcement Learning with an Infinite Mixture of Gaussian Processes

---

Mengdi Xu, Wenhao Ding, Jiacheng Zhu, Zuxin Liu, Baiming Chen, Ding Zhao

Carnegie Mellon University

{mengdixu, wenhaod, jzhu4, zuxinl, baimingc, dingzhao}@andrew.cmu.edu

## Abstract

Continuously learning to solve unseen tasks with limited experience has been extensively pursued in meta-learning and continual learning, but with restricted assumptions such as accessible task distributions, independently and identically distributed tasks, and clear task delineations. However, real-world physical tasks frequently violate these assumptions, resulting in performance degradation. This paper proposes a continual online model-based reinforcement learning approach that does not require pre-training to solve task-agnostic problems with unknown task boundaries. We maintain a mixture of experts to handle nonstationarity, and represent each different type of dynamics with a Gaussian Process to efficiently leverage collected data and expressively model uncertainty. We propose a transition prior to account for the temporal dependencies in streaming data and update the mixture online via sequential variational inference. Our approach reliably handles the task distribution shift by generating new models for never-before-seen dynamics and reusing old models for previously seen dynamics. In experiments, our approach outperforms alternative methods in non-stationary tasks, including classic control with changing dynamics and decision making in different driving scenarios. Codes available at: <https://github.com/mxu34/mbrl-gpmm>.

## 1 Introduction

Humans can quickly learn new tasks from just a handful of examples by preserving rich representations of experience [Lake et al., 2015]. Intelligent agents deployed in the real world require the same continual and quick learning ability to safely handle unknown tasks, such as navigation in new terrains and planning in dynamic traffic scenarios. Such desiderata have been previously explored in meta-learning and continual learning. Meta-learning [Sæmundsson et al., 2018, Clavera et al., 2019] achieves quick adaptation and good generalization with learned inductive bias. It assumes that the tasks for training and testing are independently sampled from the same accessible distribution. Continual learning [Chen and Liu, 2018, Nguyen et al., 2018] aims to solve a sequence of tasks with clear task delineations while avoiding catastrophic forgetting. Both communities favor Deep neural networks (DNNs) due to their strong function approximation capability but at the expense of data efficiency. These two communities are complementary, and their integration is explored in [Jerfel et al., 2019].

However, real-world physical tasks frequently violate essential assumptions of the methods as mentioned above. One example is the autonomous agent navigation problem requiring interactions with surrounding agents. The autonomous agent sequentially encounters other agents that have substantially different behaviors (e.g., aggressive and conservative ones). In this case, the mutual knowledge transfer in meta-learning algorithms may degrade the generalization performance [Deleu and Bengio, 2018]. The task distribution modeling these interactions is prohibitively complex to

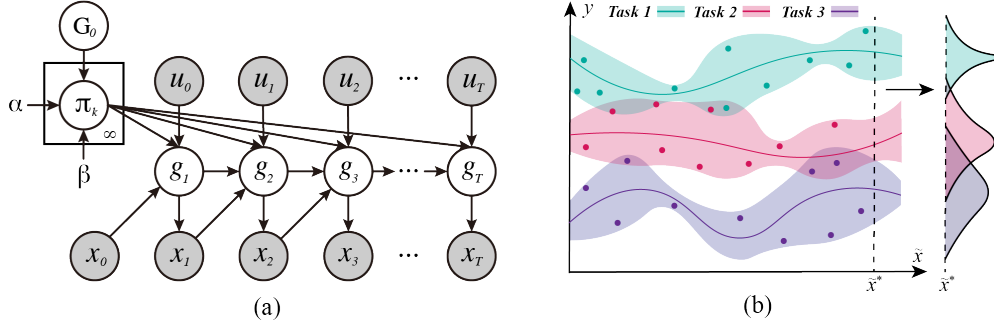


Figure 1: Method illustration. **(a)** is a graphical representation of the proposed model-based RL with an infinite mixture as the dynamics model.  $u_t$ ,  $x_t$ , and  $g_t$  represent the action, state, and the dynamics model at time  $t$ , respectively. Parameters include the concentration parameter  $\alpha$ , the base distribution  $G_0$ , and the sticky parameter  $\beta$ . **(b)** visualizes the predictive distribution at a data point  $\tilde{x}^*$ .

determine, which casts difficulties on the meta-training process with DNNs [Nagabandi et al., 2019, Vuorio et al., 2019]. Additionally, the boundaries of tasks required in most continual learning algorithms cannot feasibly be determined beforehand in an online learning setting. Although task-agnostic/task-free continual learning is explored in [Aljundi et al., 2019, Lee et al., 2020], the temporal dependencies of dynamics presented in a non-stationary robotics task are missed. For instance, two different dynamics models close together in time are likely to be related.

In this work, we aim to solve nonstationary online problems where the task boundaries and the number of tasks are unknown by proposing a model-based reinforcement learning (RL) method that does not require a pre-trained model. Model-based methods [Chua et al., 2018] are more data-efficient than model-free ones, and their performance heavily depends on the accuracy of the learned dynamics models. Similar to expansion-based continual learning methods [Jerfel et al., 2019, Yoon et al., 2018], we use an infinite mixture to model system dynamics, a graphical illustration of which is given in Figure 1 (a). It has the capacity to model an infinite number of dynamics, while the actual number is derived from the data. We represent each different type of dynamics with a Gaussian Process (GP) [Rasmussen, 2003] to efficiently leverage collected data and expressively model uncertainty. A GP is more data-efficient than a DNN (as its predictive distribution is explicitly conditioned on the collected data) and thus enables fast adaptation to new tasks even without the use of a previously trained model. With a mixture of GPs, the predictive distribution at a data point is multimodal, as shown in Figure 1 (b), with each mode representing a type of dynamics. By making predictions conditioned on the dynamics assignments, our method robustly handles dynamics that are dramatically different.

At each time step, our method either creates a new model for previously unseen dynamics or recalls an old model for encountered dynamics. After task recognition, the corresponding dynamics model parameters are updated via conjugate gradient [Gardner et al., 2018]. Considering that RL agents collect experience in a streaming manner, we learn the mixture with sequential variational inference [Lin, 2013] that is suitable for the online setting. To account for the temporal dependencies of dynamics, we propose a transition prior that stems from the Dirichlet Process (DP) prior to improve task shift detection. We select representative data points for each type of dynamics by optimizing a variational objective widely used in the Sparse GP literature [Titsias, 2009]. We demonstrate the capability of task recognition and quick task adaptation of our approach in non-stationary Cartpole-SwingUp, HalfCheetah and Highway-Intersection environments.

## 2 Related Work

Meta-learning algorithms in general consist of a base (quick) learner and a meta (slow) learner [Duan et al., 2016, Wang et al., 2016] and have recently been combined with RL to solve nonstationary problems via model-free [Finn et al., 2017, Houthoofd et al., 2018, Rothfuss et al., 2019] and model-based approaches [Clavera et al., 2019, Sæmundsson et al., 2018]. The closest work to our research is [Nagabandi et al., 2019], which uses a mixture of DNNs as the dynamics model in model-based RL but still requires a model-agnostic meta-learning (MAML) prior. Researchers in [Vuorio et al.,

2019] augment MAML with a multimodal task distribution for solving substantially different tasks. However, it inherits the limitations of MAML (such as assuming accessible task simulations and clear task boundaries). Additionally, the meta training strategy increases sample complexity and thus makes many model-free meta-learning algorithms infeasible to implement on real-world problems [Peters and Schaal, 2008]. Using a single GP as the dynamics model in model-based meta-RL is explored in [Sæmundsson et al., 2018] by updating latent variables for different tasks but in an offline and episodic setting. To the best of our knowledge, our method is the first capable of robustly handling online nonstationary tasks without requiring task delineations or depending on a pre-trained model.

Using a mixture of experts to solve different tasks is explored in continual learning [Wilson et al., 2007, Chen and Liu, 2018, Candy, 1991] and Multi-task Learning [Ruder, 2017, Evgeniou and Pontil, 2004, Jacob et al., 2009]. However, previous works from both communities require clear task delineations. The conventional inference methods for mixture models mainly consist of MCMC sampling [Jain and Neal, 2004, Dahl, 2005] and variational inference [Blei et al., 2006]. Both methods keep the information of the whole dataset and do inference iteratively via multiple passes. In contrast, streaming variational inference [Broderick et al., 2013, Huynh et al., 2016, Tank et al., 2015] for Bayesian nonparametric models is designed for handling streaming data and requires a single computation pass. Sequential variational inference [Lin, 2013] for DP mixtures has been recently integrated with DNNs for image classification [Lee et al., 2020].

### 3 Model-Based RL with an Infinite Mixture of Gaussian Processes

Model-based RL algorithms rely on the learned dynamics model to roll out environments. For real-world tasks that contain substantially different dynamics, using an infinite mixture model as the dynamics model alleviates the harmful mutual knowledge transfer when using a single model, and enables the backward transfer of knowledge by recalling and updating stored dynamics models. Learning the system dynamics model  $f$  is carried out by performing inference on data-efficient GPs to avoid training a prior model as in [Jerfel et al., 2019, Nagabandi et al., 2019]. Additionally, GPs define distributions over functions and thus naturally capture the aleatoric uncertainty of noisy environments. We use Model Predictive Control (MPC) for selecting an action at each time step, which can be seen as a closed-loop controller and increases robustness to model errors.

We consider the system dynamics model in the form of  $\mathbf{x}_{t+1} = \mathbf{x}_t + f(\mathbf{x}_t, \mathbf{u}_t)$ . The input is augmented as  $\tilde{\mathbf{x}}_t = (\mathbf{x}_t, \mathbf{u}_t)$ , where  $\mathbf{x}_t \in \mathbb{R}^c$  and  $\mathbf{u}_t \in \mathbb{R}^d$  are the state and action at time  $t$ , respectively. The target  $\mathbf{y}_t = \Delta \mathbf{x}_t = \mathbf{x}_{t+1} - \mathbf{x}_t$  is the state increment. A history dataset  $\mathcal{D} = \{\tilde{\mathbf{x}}^j, \mathbf{y}^j\}_{j=1}^m$  is maintained to update the mixture model and predict increments in MPC. The inputs and targets are aggregated into  $\tilde{X} \in \mathbb{R}^{(c+d) \times m}$  and  $Y \in \mathbb{R}^{c \times m}$ . With each dynamics model as a GP [Rasmussen, 2003], the dynamics function  $f$  can be decoupled by dimension as  $f = (f_1, \dots, f_c)$  with  $f_i : \mathbb{R}^c \rightarrow \mathbb{R}$ . The state difference given a new observation  $\mathbf{x}$  and action  $\mathbf{u}$  is drawn from the predictive distribution

$$p(f|\mathcal{D}, \tilde{\mathbf{x}}_t) = \prod_{i=1}^c \mathcal{N}(m(f_i), \text{cov}(f_i)). \quad (1)$$

The mean function is  $m(f_i) = K_i(\tilde{\mathbf{x}}, \tilde{X})[K_i(\tilde{X}, \tilde{X}) + \sigma_i^2 I]^{-1} Y^i$  and the covariance matrix is  $\text{cov}(f_i) = K_i(\tilde{\mathbf{x}}, \tilde{\mathbf{x}}) - K_i(\tilde{\mathbf{x}}, \tilde{X})[K_i(\tilde{X}, \tilde{X}) + \sigma_i^2 I]^{-1} K_i(\tilde{X}, \tilde{\mathbf{x}})$ .  $Y^i$  denotes the target's  $i$ th dimension.  $\sigma_i$  is the standard deviation of observation noise of dimension  $i$ . The matrix  $K_i$  is fully specified by the kernel function  $k_i(\tilde{\mathbf{x}}, \tilde{\mathbf{x}}_*)$ , which defines the function smoothness. For simplicity, we use the scaled squared exponential kernel  $k_i(\tilde{\mathbf{x}}, \tilde{\mathbf{x}}_*) = w_i^2 \exp(-\frac{1}{2} \sum_{j=1}^{c+d} w_{i,j} (\tilde{\mathbf{x}}^j - \tilde{\mathbf{x}}_*^j)^2)$ .  $w_{i,j}$  is the reciprocal of the lengthscale between dimensions  $i$  and  $j$ , and  $w_i$  is the output scale of dimension  $i$ .

### 4 Scalable Online Bayesian Inference

This section presents a scalable online Bayesian inference method for learning an infinite mixture of GPs in the model-based RL setting. We assume that it is possible for a new type of dynamics to emerge at every timestep, and the total number of different dynamics is unknown. We observe a new data pair  $(\mathbf{x}_t, \mathbf{u}_t, \Delta \mathbf{x}_t)$  each time  $t$  the RL agent interacts with the environment. To learn the mixture model, we first identify the latent dynamics assignment variable  $z_t$  and then update the

---

**Algorithm 1:** Bayesian Inference for Continual Online Model-based Reinforcement Learning

---

**Input:** Concentration parameter  $\alpha$ , Initial parameter  $\theta_0$ , Sticky parameter  $\beta$ , KL threshold  $\epsilon$ ,

Merge trigger  $n_{merge}$ , Data Distillation trigger  $n_{distill}$ , Inducing point number  $m$

**Output:** Infinite Mixture Model  $M$ , Representative Dataset  $\mathcal{D}$

Initialization:  $M \leftarrow \{M_0\}$ ,  $\mathcal{D} \leftarrow \{\emptyset\}$ ,  $t \leftarrow 0$ ,  $z_0 \leftarrow 0$ , and  $K \leftarrow 1$ ;

$(\mathbf{x}_0, \mathbf{u}_0, \Delta \mathbf{x}_0) \leftarrow RandomPolicy$ ;

$\mathcal{D} \leftarrow \mathcal{D} \cup \{(z_0, \mathbf{x}_0, \mathbf{u}_0, \Delta \mathbf{x}_0)\}$ ;

Update  $\theta_0$  with (4);

**while** *task not finish* **do**

$z_{old} \leftarrow z_t$ ,  $t \leftarrow t + 1$ ;

$(\mathbf{x}_t, \mathbf{u}_t, \Delta \mathbf{x}_t) \leftarrow MPC(M_{z_{t-1}})$ ;

    // Sequential Variational Inference with Transition Prior  
    (Section 4.1)

    Update  $q_t^{pr}(z_t)$  with (3);

    Update  $z_t = \operatorname{argmax}_k \rho_t(z_{tk})$  with (2);

**if**  $z_t = K$  **then**

        Append  $M_{z_t}$  to  $M$ ,  $K \leftarrow K + 1$

$\mathcal{D} \leftarrow \mathcal{D} \cup \{(z_t, \mathbf{x}_t, \mathbf{u}_t, \Delta \mathbf{x}_t)\}$ ;

    Update  $\theta_{z_t}$  with (4);

    // Expert Merge and Prune (Section 4.3)

**if**  $\sum_{i=0}^t \mathbf{1}\{z_i = z_t\} = n_{merge}$  **then**

$d_t(k) = d(M_{z_t}, M_k)$ ,  $k = 0, \dots, K - 1$  with (6);

**if**  $\min_k d_t \leq \epsilon$  **then**

            Merge  $M_{z_t}$  to the most similar model  $M_{\operatorname{arg\,min}_k d_t}$ ,  $K \leftarrow K - 1$

**if**  $\sum_{i=0}^t \mathbf{1}\{z_i = z_{old}\} \leq n_{merge}$  **and**  $z_t \neq z_{old}$  **then**

        Merge  $M_{z_t}$  to the most similar adjacent model based on  $d(M_{z_t}, M_k)$ ,  $K \leftarrow K - 1$

    // Data Distillation (Section 4.2)

**if**  $\sum_{i=0}^t \mathbf{1}\{z_i = k\} \geq n_{distill}$ ,  $\forall k$  **then**

        Get  $m$  inducing points with (5)

---

dynamics-specific parameters  $\theta_{z_t}$  of expert  $M_{z_t}$ . Our goal is to jointly do inference over  $z$  and learn  $\theta$  in an online streaming setting by maximizing the log posterior probability given the observed data  $p_n(z_{1:n}, \theta | \mathcal{D})$ . To get a reasonable action at time  $t + 1$ , with the inferred dynamics assignment  $z_t$ , we select the expert  $M_{z_t}$  to generate predictions  $\mathbf{y}_{t+1:t+T}$  for the MPC.

We first introduce sequential variational inference with transition prior in Section 4.1. To make our model scalable to large datasets, we introduce an optimization-based method in Section 4.2 to eliminate redundant data points. The stability of the mixture model is enhanced by merging similar experts and pruning redundant ones, as in Section 4.3. We present the overall pipeline in Algorithm 1 and discuss the effect of model parameters in Section S2 in the supplementary material.

#### 4.1 Sequential Variational Inference with Transition Prior

We approximate the intractable  $p_n(z_{0:n}, \theta | \mathcal{D})$  as  $\hat{q}_n(z_{0:n}, \theta) = \prod_{k=0}^{\infty} \gamma_n(\theta_k) \prod_{i=0}^n \rho_n(z_i)$  using Assumed Density Filtering (ADF) and mean field approximation. As derived in [Tank et al., 2015], the optimal distribution of the dynamics assignment  $z_n$  of the  $n$ th observation is

$$\rho_n(z_{nk}) \propto \begin{cases} q^{pr}(z_{nk}) \int p((\tilde{\mathbf{x}}_n, \mathbf{y}_n) | \theta_k) \gamma_{n-1}(\theta_k) d\theta_k & 0 \leq k \leq K_{n-1} - 1 \\ q^{pr}(z_{nk}) \int p((\tilde{\mathbf{x}}_n, \mathbf{y}_n) | \theta_k) G_0(\theta_k) d\theta_k & k = K_{n-1} \end{cases} \quad (2)$$

where  $q^{pr}(z_n) = \sum_{z_{0:n-1}} p(z_n | z_{0:n-1}) \prod_{i=0}^{n-1} \rho_{n-1}(z_i)$ , and  $G_0$  is the base distribution for dynamics-specific parameter  $\theta$ .  $q^{pr}$  acts as the prior probability of the assignments and is analogous to the predictive rule  $p(z_n | z_{0:n-1})$ .  $G_0$  and  $\gamma_{n-1}$  in general are in the same exponential family as  $\rho_n(z_n)$  so that (2) is in closed form. When using a DP mixture model,  $q^{pr}$  is in the form of the Chinese Restaurant Process prior. The sequential variational inference method for DP mixtures [Lin, 2013] is suitable for dealing with streaming data with overall complexity  $O(NK)$ , where  $N$  is the number of data points and  $K$  is the expected number of experts.

However, in the task-agnostic setting where the task assignment is evaluated at each time step, dynamics models are not independently sampled from a prior. Instead, the adjacent observations tend to belong to the same dynamics model, and there may exist temporal transition dependencies between different dynamics models. Therefore, we adopt the Markovian assumption when selecting the assignment prior  $q_n^{pr}$  and propose a transition prior that conditions on the previous data point's dynamics assignment  $z_{n-1}$  as follows:

$$q_n^{pr} \propto \begin{cases} \sum_{i=1}^n \mathbf{1}\{z_{i-1} = z_{n-1}\} \rho_i(z_{ik}) + \mathbf{1}\{k = z_{n-1}\} \beta, & 0 \leq k \leq K_{n-1} - 1 \\ \alpha, & k = K_{n-1} \end{cases} \quad (3)$$

Here  $\beta$  is the sticky parameter that increases the probability of self-transition to avoid rapidly switching between dynamics models [Fox et al., 2011]. Note that in Algorithm 1, we approximate the soft dynamics assignment  $\rho_i(z_{ik})$  of the  $i$ th data pair with the hard assignment  $z_i = \operatorname{argmax}_k \rho_i(z_{ik})$ . The argmax/hard assignment approximation splits the streaming data and thus accelerates the stochastic update of model parameters and simplifies the form of transition prior. However, this involves a trade-off [Kearns et al., 1998] between how well the data are balanced and the density accuracy.

For GPs,  $\theta$  is a set of kernel parameters  $\{w_i, w_{i,1}, \dots, w_{i,c}, \sigma_i\}_{i=1}^c$ . Since it is hard to find a conjugate prior  $G_0$  for  $\theta$ , and we are considering a task-agnostic setting with limited prior knowledge, we use the likelihood  $F((\tilde{\mathbf{x}}_n, \mathbf{y}_n) | \theta_k)$  to approximate the integrals in (2), inspired by the auxiliary variable approach [Neal, 2000]. In order to create a GP expert for unobserved dynamics, we need to find the likelihood of a GP with no data [Rasmussen and Ghahramani, 2002]. Therefore, we initialize the kernel of the first GP dynamics model  $M_0$  with a fixed reasonable point estimation  $\theta_{init}$  to evaluate the likelihood conditional on it. We then train a global GP dynamics model with all online collected data and use the updated parameters as the prior when initializing succeeding GP experts. To deal with the non-conjugate situation, we use stochastic batch optimization and update  $\theta$  with (4).

$$\theta_k \leftarrow \theta_k - \eta \sum_{i=0}^n \mathbf{1}\{z_i = k\} \nabla_{\theta} \log p(\mathbf{y}_i | \tilde{\mathbf{x}}_i, \mathcal{D}, \theta_k), \quad \forall k = 0, \dots, K_n - 1 \quad (4)$$

Note that the iterative updating procedure of dynamics assignment  $z$  and dynamics-specific parameters  $\theta$  can be formulated as a variational expectation-maximization (EM) algorithm. In the variational E step, we calculate the soft assignment, which is the posterior probability conditioned on the dynamics parameters  $\theta$ . In the M step, given each data pair's assignment, we update  $\theta$  for each dynamics model with the conjugate gradient method to maximize the log-likelihood.

## 4.2 Data Distillation with Inducing Points

GP dynamics models need to retain a dataset  $\mathcal{D}$  for training and evaluation, for which the spatial and computational complexity increases as more data is accumulated. For instance, the prediction complexity in (1) is  $O(N_k^3)$  due to the matrix inversion. To make the algorithm computationally tractable, we select a non-growing but large enough number of data points that contain maximum information to balance the tradeoff between algorithm complexity and model accuracy. In a model-based RL setting, the data distillation procedure is rather critical since the agent exploits the learned dynamics models frequently to make predictions in MPC, and thus the overall computational load heavily depends on the prediction complexity.

For each constructed dynamics model  $k$ , data distillation is triggered if the number of data points belonging to  $M_k$  reaches a preset threshold  $n_{distill}$ . Define  $\mathcal{D}_k = \{(z_i, \mathbf{x}_i, \mathbf{u}_i, \Delta \mathbf{x}_i) | z_i = k\}$ . The  $m$  inducing points  $\mathcal{D}_{k,m}$  are selected while preserving the posterior distribution over  $f$  as in exact GP in (1) by maximizing the following lower bound that is widely used in Sparse GP literature [Titsias, 2009, Tran et al., 2015]:

$$L = \sum_{i=1}^c \left[ \log \mathcal{N}(Y^i; 0, K_{nm} K_{mm}^{-1} K_{mn} + I \sigma_i^2) - \frac{1}{2\sigma_i^2} \operatorname{Tr}(K_{nn} - K_{nm} K_{mm}^{-1} K_{mn}) \right] \quad (5)$$

Note that the collected data depends on the learned dynamics model and the rolled-out policy, which introduces a nonstationary data distribution. In addition to the setting that the GP experts are trained online from scratch, treating inducing points as pseudo-points and optimizing (5) via continuous optimization may lead to an unstable performance in the initial period. Instead, we directly construct  $\mathcal{D}_{k,m}$  by selecting real data points from  $\mathcal{D}_k$  via Monte Carlo methods. Other criteria and optimization methods for selecting inducing points can be found in [Titsias et al., 2019].

### 4.3 Expert Merge and Prune

Since each data point’s dynamics assignment is only evaluated once, dynamics models may be incorrectly established, especially in early stages where the data numbers of existing dynamics models are relatively small. Redundant dynamics models not only harm the prediction performance by blocking the forward and backward knowledge transfer but also increase the computational complexity when calculating  $z$  (which requires iterating over the mixture). Therefore, we propose to merge redundant models and prune unstable ones with linear complexity w.r.t. the number of spawned dynamics models. Other methods for merging experts can be found in [Guha et al., 2019].

**Expert merging mechanism.** We say that a newly constructed dynamics model  $M_K$  is in a burn-in stage if the number of data points belonging to it is less than a small preset threshold  $n_{merge}$ . At the end of the burn-in stage, we check the distances between  $M_K$  with the older models. If the minimum distance obtained with  $M_{k'}$  is less than the threshold  $\epsilon$ , we merge the new model  $M_K$  by changing the assignments of data in  $\mathcal{D}_K$  to  $z = k'$ . We use the KL-divergence between the predictive distributions evaluated at  $\mathcal{D}_K$  conditioned on two dynamics models as the distance metric:

$$d(M_K, M_k) = \sum_{i \in \mathcal{D}_K} KL(p(f|\mathcal{D}_k, \tilde{\mathbf{x}}_i) || p(f|\mathcal{D}_K, \tilde{\mathbf{x}}_i)) \tag{6}$$

**Expert pruning method.** We assume that in real-world situations, each type of dynamics lasts for a reasonable period. If a dynamics model  $M_K$  accumulates data less than the merge trigger  $n_{merge}$  when a new dynamics model is spawned, we treat  $M_K$  as an unstable cluster and merge it with adjacent dynamics models based on the distance in (6).

## 5 Experiments: Task-Agnostic Online Model-Based RL

We present experiments in this section to investigate whether the proposed method (i) detects the change points of the dynamics given the streaming data, (ii) improves task detection performance by using the transition prior, (iii) automatically initializes new models for never-before-seen dynamics and identifies previously seen dynamics, and (iv) achieves equivalent or better task performance than baseline models while using only a fraction of their required data.

We use three non-stationary environments for our experiments, as shown in Figure 2. In each environment, the RL agent cyclically encounters several different types of dynamics. In Cartpole-SwingUp, we aim to swing the pole upright meanwhile keep the cart in the middle. The pole length  $l$  and mass  $m$  vary sequentially by alternating between four different combinations. HalfCheetah is a more complex control problem having larger state and control dimensions with the non-stationary dynamics induced by different torso loads. The goal is to make the half cheetah run as fast as possible. Highway-Intersection contains surrounding vehicles with different target destinations, and the ego vehicle needs to avoid collisions while heading to its goal. More detailed experiment settings are presented in Section S1 in the supplementary material.

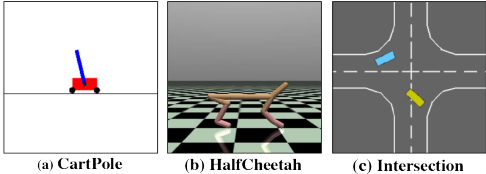


Figure 2: Simulation environments

We compare our method with five model-based baselines detailed as follows:

- (a) **Single dynamics model:** We investigate the task performance of using a GP, a DNN, and an Attentive Neural Process (ANP) [Kim et al., 2019, Qin et al., 2019] as the dynamics model. The GP is trained online from scratch, while the ANP and the DNN are first trained offline with data pre-collected in all dynamics that the agent may encounter online. All three models are updated online to account for the non-stationarity of environments after each batch of data is collected.
- (b) **Mixture of DNNs:** We compare with another two pre-trained baselines using mixtures of DNNs as the dynamics model with DP prior (DPDNN) and the proposed transition prior (T-DNN), respectively. Considering that our method does not require an adaptation module for updating model parameters, we directly use the weights of a global DNN that is trained

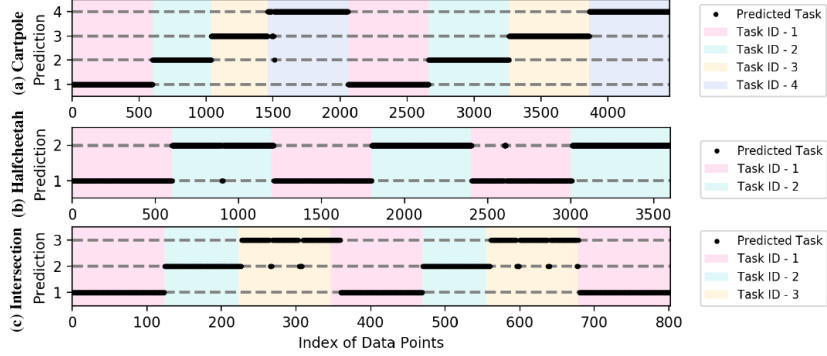


Figure 3: Dynamics assignments with the proposed transition prior. Our method successfully detects the dynamics shift. It allocates new components to model previously unseen types of dynamics and recalls stored models when encountering seen dynamics.

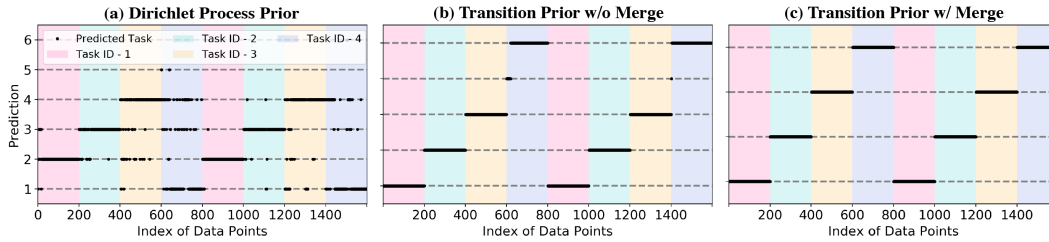


Figure 4: Ablation experiment results of the transition prior as well as the merge and prune mechanism in `Cartpole-SwingUp`. The proposed transition prior achieves more accurate dynamics assignments than the DP prior. The merge and prune mechanism successfully merges redundant dynamics models.

with all collected data as the prior instead of using a MAML-trained prior as in [Nagabandi et al., 2019].

- (c) **Meta-RL**: We use the MAML algorithm [Finn et al., 2017] to learn the dynamics model for model-based RL. After being pre-trained with several episodes, the meta-model is adapted online with recently collected data to deal with nonstationarity.

### 5.1 Task Switching Detection

In all three environments that contain sudden switches between different dynamics, our method detects the task distribution shift as visualized in Figure 3. In general, the predicted region of each type of dynamics matches that of the ground truth. We notice that there exists some delay when detecting change points and hypothesize that this may be due to the clustering property and sticky mechanism of the transition prior. Although DPs [Teh, 2010] have the so-called rich-gets-richer property, directly using a DP prior fails to capture the temporal relationship between data points and thus leads to inaccurate dynamics assignments (Figure 4 (a)). We also notice that wrong dynamics assignments result in unstable task performances with smaller rewards and larger variances, as shown in Section S3. There are some redundant dynamics models during online training (Figure 4 (b)) when not using the merge and prune mechanism. When comparing Figure 4 (b) and (c), we can see that our method successfully merges redundant dynamics models to the correct existing ones.

### 5.2 Task Performance

We evaluate the task performance in terms of the accumulated rewards for each type of dynamics, as displayed in Figure 5. Since a separate model is initialized and trained from scratch whenever a new type of dynamics is detected, our method’s reward oscillates during the initial period after the dynamics shift (especially in Figure 5 (a)). However, our method performs well in a new type of dynamics after collecting just a handful of data points that are far less than DNN-based methods. For example, for each type of dynamics in `Cartpole-SwingUp`, our method converges after collecting

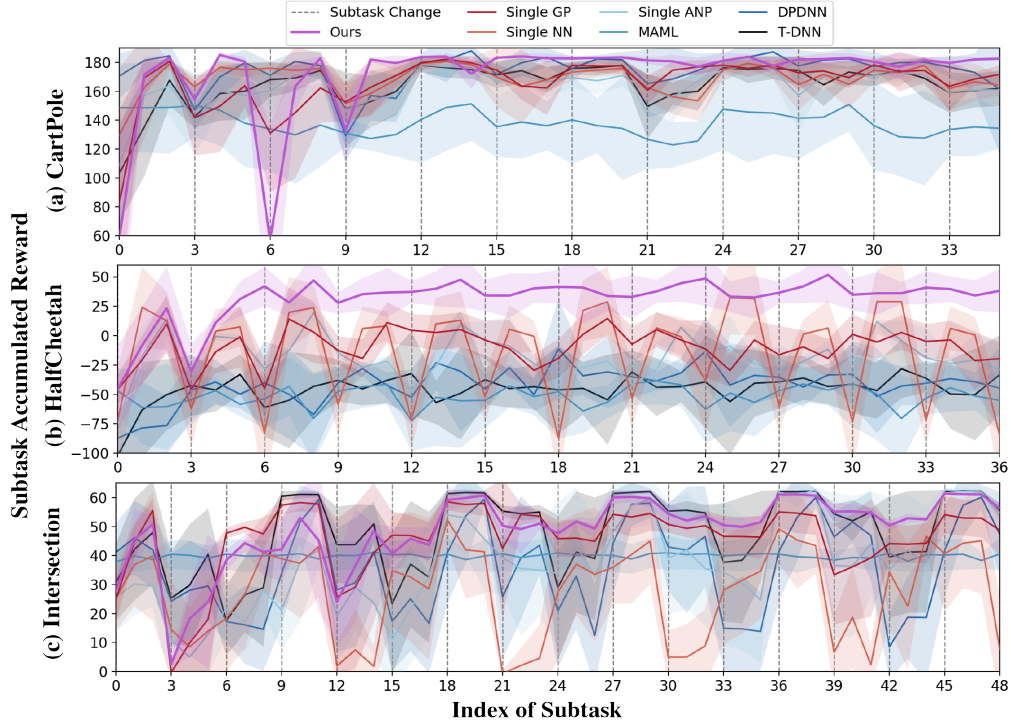


Figure 5: Accumulated rewards in three nonstationary environments. A subtask is analogous to an episode. Each vertical dotted line indicates a dynamics switch. Our method is more robust, data-efficient, and has higher rewards.

600 data points, while DNN may need around 1500 data points [Chua et al., 2018]. By learning the latent dynamics assignment, our method quickly adapts when it encounters previously seen dynamics by shifting to the corresponding dynamics model. These previously learned models are further improved by being updated with the newly collected data according to their dynamics assignments. Additionally, our method is more robust than all the baselines and has a smaller variance at convergence.

Using a single dynamics model automatically preserves global dynamics properties. Therefore using a single GP without pre-training does not suffer apparent performance degradation when the dynamics switch. Since both the DNN and the ANP use pre-trained models, they achieve equivalent (in complex Highway-Intersection) or better (in simple Cartpole-SwingUp) performance as our method when encountering new dynamics. However, the three single dynamics model baselines fail to consistently succeed and oscillate a lot as the environment getting more complex. For example, when using a DNN in the unprotected left-turn scenario in Highway-Intersection, the RL agent keeps colliding with the other vehicle. Although the ANP is a DNN approximation of the GP and can deal with multiple tasks itself [Galashov et al., 2019], its performance still oscillates, and thus it cannot robustly handle the multimodal task distribution. The online adaptation mechanism causes the single model to tend to overfit to the current dynamics. The overfitting problem further harms the quick generalization performance since the adjacent dynamics are substantially different, and previously adapted model parameters may be far from the optimal ones for the new dynamics. Additionally, without task recognition, the model suffers from the forgetting problem due to not retaining data and parameters of previously seen dynamics.

Figure 5 also show that our method outperforms the three baselines that aim to handle nonstationarity. The model-based RL with MAML is easily trapped in local minima determined by the meta-prior. For instance, the RL agent in Highway-Intersection learns to turn in the right direction but fails to drive to the right lane. In our experiments, MAML also cannot quickly adapt to substantially different dynamics. This is because MAML suffers when a unimodal task distribution is not sufficient to represent encountered tasks. The model-based RL with a DP mixture of DNNs performs slightly



better than a single DNN but still oscillates due to inaccurate task assignments, as in Section S3. T-DNN performs similarly to DPDNN and still underperforms our method due to the inaccuracy of DNN model predictions with limited data.

## 6 Discussion

We propose a scalable online model-based RL method with an infinite mixture of GPs to handle real-world task-agnostic situations with limited prior knowledge. Our method achieves quick adaptation and avoids pre-training by using data-efficient GPs as dynamics models and avoids catastrophic forgetting by retaining a mixture of experts. Our model performs well when dynamics are substantially different by constructing a multimodal predictive distribution and blocking harmful knowledge transfer via task recognition. We propose a transition prior to explicitly model the temporal dependency and thus release the assumption that tasks are independent and identically distributed. Additionally, our method detects the dynamics shift at each time step, so it is suitable for situations with unknown task delineations. We learn the mixture via online sequential variational inference that is scalable to extensive streaming data with data distillation and the merge and prune technique. Since computing the posterior of a GP becomes intractable as the data size and data dimension increase, replacing GPs with Neural Processes [Kim et al., 2019, Garnelo et al., 2018] would be an interesting direction to explore. Another direction would be to incorporate meta-learning into our method to better leverage the commonly shared information across the different dynamics.

### Broader Impact

This work is a step toward General Artificial Intelligence by eliminating the pre-train stage and equipping reinforcement learning agents with the quick-adaptation ability. The proposed method could be applied in a wide range of applications when the prior knowledge is not accessible or not beneficial, including space rover navigation, rescue robot exploration, autonomous vehicle decision making, and human-robot interaction.

Our research increases algorithmic interpretability and transparency for decision-making by providing inferred task assignments. It also enhances the algorithm’s robustness by explicitly separating different types of tasks and thus increases users’ trust. Additionally, our research improves algorithmic fairness by not relying on prior knowledge that may contain human-induced or data-induced biases. At the same time, our research may have negative impacts if misused. The potential risks are listed as follows: (1) Over-trust in the results (e.g., the task assignments) may lead to undesirable outcomes. (2) If used for illegal purposes, the model may instead enlarge the possible negative outcome due to its explainability. (3) The task assignment results may be misinterpreted by those who do not have enough related background. (4) The evolving online nature of the method may increase the uncertainty and thus mistrust of human collaborators. Note that our method inherits the possible positive and negative impacts of reinforcement learning, not emphasized here.

To mitigate the possible risks mentioned above, we encourage research to (1) investigate and modulate the negative impacts of the inaccurate information provided by algorithms, (2) understand how humans interact with evolving intelligent agents in terms of trust, productivity, comfort level, (3) find out the impact of using our model in real-world tasks.

### Acknowledgments and Disclosure of Funding

Thanks go to Mr. Keegan Harris for revision and advice. The authors gratefully acknowledge the support from the Manufacturing Futures Initiative at Carnegie Mellon University, made possible by the Richard King Mellon Foundation. The ideas presented are solely those of the authors.

### References

- Brenden M Lake, Ruslan Salakhutdinov, and Joshua B Tenenbaum. Human-level concept learning through probabilistic program induction. *Science*, 350(6266):1332–1338, 2015.
- Steindór Sæmundsson, Katja Hofmann, and Marc Peter Deisenroth. Meta reinforcement learning with latent variable gaussian processes. In *Conference on Uncertainty in Artificial Intelligence*

- (UAI), May 2018. URL <https://www.microsoft.com/en-us/research/publication/meta-reinforcement-learning-latent-variable-gaussian-processes/>.
- Ignasi Clavera, Anusha Nagabandi, Simin Liu, Ronald S. Fearing, Pieter Abbeel, Sergey Levine, and Chelsea Finn. Learning to adapt in dynamic, real-world environments through meta-reinforcement learning. In *International Conference on Learning Representations*, 2019. URL <https://openreview.net/forum?id=HyztsoC5Y7>.
- Zhiyuan Chen and Bing Liu. Lifelong machine learning. *Synthesis Lectures on Artificial Intelligence and Machine Learning*, 12(3):1–207, 2018.
- Cuong V. Nguyen, Yingzhen Li, Thang D. Bui, and Richard E. Turner. Variational continual learning. In *International Conference on Learning Representations*, 2018. URL <https://openreview.net/forum?id=BkQqq0gRb>.
- Ghassen Jerfel, Erin Grant, Tom Griffiths, and Katherine A Heller. Reconciling meta-learning and continual learning with online mixtures of tasks. In *Advances in Neural Information Processing Systems*, pages 9119–9130, 2019.
- Tristan Deleu and Yoshua Bengio. The effects of negative adaptation in model-agnostic meta-learning. *arXiv preprint arXiv:1812.02159*, 2018.
- Anusha Nagabandi, Chelsea Finn, and Sergey Levine. Deep online learning via meta-learning: Continual adaptation for model-based RL. In *International Conference on Learning Representations*, 2019. URL <https://openreview.net/forum?id=HyxAfnA5tm>.
- Risto Vuorio, Shao-Hua Sun, Hexiang Hu, and Joseph J Lim. Multimodal model-agnostic meta-learning via task-aware modulation. In *Advances in Neural Information Processing Systems*, pages 1–12, 2019.
- Rahaf Aljundi, Klaas Kelchtermans, and Tinne Tuytelaars. Task-free continual learning. In *Proceedings of the IEEE Conference on Computer Vision and Pattern Recognition*, pages 11254–11263, 2019.
- Soochan Lee, Junsoo Ha, Dongsu Zhang, and Gunhee Kim. A neural dirichlet process mixture model for task-free continual learning. In *International Conference on Learning Representations*, 2020. URL <https://openreview.net/forum?id=SJxS0JStPr>.
- Kurtland Chua, Roberto Calandra, Rowan McAllister, and Sergey Levine. Deep reinforcement learning in a handful of trials using probabilistic dynamics models. In *Advances in Neural Information Processing Systems*, pages 4754–4765, 2018.
- Jaehong Yoon, Eunho Yang, Jeongtae Lee, and Sung Ju Hwang. Lifelong learning with dynamically expandable networks. In *International Conference on Learning Representations*, 2018. URL <https://openreview.net/forum?id=Sk7KsfW0->.
- Carl Edward Rasmussen. Gaussian processes in machine learning. In *Summer School on Machine Learning*, pages 63–71. Springer, 2003.
- Jacob Gardner, Geoff Pleiss, Kilian Q Weinberger, David Bindel, and Andrew G Wilson. Gpytorch: Blackbox matrix-matrix gaussian process inference with gpu acceleration. In *Advances in Neural Information Processing Systems*, pages 7576–7586, 2018.
- Dahua Lin. Online learning of nonparametric mixture models via sequential variational approximation. In *Advances in Neural Information Processing Systems*, pages 395–403, 2013.
- Michalis Titsias. Variational learning of inducing variables in sparse gaussian processes. In *Artificial Intelligence and Statistics*, pages 567–574, 2009.
- Yan Duan, John Schulman, Xi Chen, Peter L Bartlett, Ilya Sutskever, and Pieter Abbeel. RL2: Fast reinforcement learning via slow reinforcement learning. *arXiv preprint arXiv:1611.02779*, 2016.
- Jane X Wang, Zeb Kurth-Nelson, Dhruva Tirumala, Hubert Soyer, Joel Z Leibo, Remi Munos, Charles Blundell, Dharshan Kumaran, and Matt Botvinick. Learning to reinforcement learn. *arXiv preprint arXiv:1611.05763*, 2016.

- Chelsea Finn, Pieter Abbeel, and Sergey Levine. Model-agnostic meta-learning for fast adaptation of deep networks. In *Proceedings of the 34th International Conference on Machine Learning-Volume 70*, pages 1126–1135. JMLR. org, 2017.
- Rein Houthoofd, Yuhua Chen, Phillip Isola, Bradly Stadie, Filip Wolski, OpenAI Jonathan Ho, and Pieter Abbeel. Evolved policy gradients. In *Advances in Neural Information Processing Systems*, pages 5400–5409, 2018.
- Jonas Rothfuss, Dennis Lee, Ignasi Clavera, Tamim Asfour, and Pieter Abbeel. ProMP: Proximal meta-policy search. In *International Conference on Learning Representations*, 2019. URL <https://openreview.net/forum?id=SkxXCi0qFX>.
- Jan Peters and Stefan Schaal. Reinforcement learning of motor skills with policy gradients. *Neural networks*, 21(4):682–697, 2008.
- Aaron Wilson, Alan Fern, Soumya Ray, and Prasad Tadepalli. Multi-task reinforcement learning: a hierarchical bayesian approach. In *Proceedings of the 24th international conference on Machine learning*, pages 1015–1022, 2007.
- Philip C Candy. *Self-Direction for Lifelong Learning. A Comprehensive Guide to Theory and Practice*. ERIC, 1991.
- Sebastian Ruder. An overview of multi-task learning in deep neural networks. *arXiv preprint arXiv:1706.05098*, 2017.
- Theodoros Evgeniou and Massimiliano Pontil. Regularized multi-task learning. In *Proceedings of the tenth ACM SIGKDD international conference on Knowledge discovery and data mining*, pages 109–117, 2004.
- Laurent Jacob, Jean-philippe Vert, and Francis R Bach. Clustered multi-task learning: A convex formulation. In *Advances in neural information processing systems*, pages 745–752, 2009.
- Sonia Jain and Radford M Neal. A split-merge markov chain monte carlo procedure for the dirichlet process mixture model. *Journal of computational and Graphical Statistics*, 13(1):158–182, 2004.
- David B Dahl. Sequentially-allocated merge-split sampler for conjugate and nonconjugate dirichlet process mixture models. *Journal of Computational and Graphical Statistics*, 11(6), 2005.
- David M Blei, Michael I Jordan, et al. Variational inference for dirichlet process mixtures. *Bayesian analysis*, 1(1):121–143, 2006.
- Tamara Broderick, Nicholas Boyd, Andre Wibisono, Ashia C Wilson, and Michael I Jordan. Streaming variational bayes. In *Advances in neural information processing systems*, pages 1727–1735, 2013.
- Viet Huynh, Dinh Phung, and Svetha Venkatesh. Streaming variational inference for dirichlet process mixtures. In *Asian Conference on Machine Learning*, pages 237–252, 2016.
- Alex Tank, Nicholas Foti, and Emily Fox. Streaming variational inference for bayesian nonparametric mixture models. In *Artificial Intelligence and Statistics*, pages 968–976, 2015.
- Emily B Fox, Erik B Sudderth, Michael I Jordan, and Alan S Willsky. A sticky hdp-hmm with application to speaker diarization. *The Annals of Applied Statistics*, pages 1020–1056, 2011.
- Michael Kearns, Yishay Mansour, and Andrew Y Ng. An information-theoretic analysis of hard and soft assignment methods for clustering. In *Learning in graphical models*, pages 495–520. Springer, 1998.
- Radford M Neal. Markov chain sampling methods for dirichlet process mixture models. *Journal of computational and graphical statistics*, 9(2):249–265, 2000.
- Carl E Rasmussen and Zoubin Ghahramani. Infinite mixtures of gaussian process experts. In *Advances in neural information processing systems*, pages 881–888, 2002.

- Dustin Tran, Rajesh Ranganath, and David M Blei. The variational gaussian process. *arXiv preprint arXiv:1511.06499*, 2015.
- Michalis K Titsias, Jonathan Schwarz, Alexander G de G Matthews, Razvan Pascanu, and Yee Whye Teh. Functional regularisation for continual learning with gaussian processes. In *International Conference on Learning Representations*, 2019.
- Aritra Guha, Nhat Ho, and XuanLong Nguyen. On posterior contraction of parameters and interpretability in bayesian mixture modeling. *arXiv preprint arXiv:1901.05078*, 2019.
- Hyunjik Kim, Andriy Mnih, Jonathan Schwarz, Marta Garnelo, Ali Eslami, Dan Rosenbaum, Oriol Vinyals, and Yee Whye Teh. Attentive neural processes. In *International Conference on Learning Representations*, 2019. URL <https://openreview.net/forum?id=SkE6PjC9KX>.
- Shenghao Qin, Jiacheng Zhu, Jimmy Qin, Wenshuo Wang, and Ding Zhao. Recurrent attentive neural process for sequential data. *arXiv preprint arXiv:1910.09323*, 2019.
- Yee Whye Teh. Dirichlet process., 2010.
- Alexandre Galashov, Jonathan Schwarz, Hyunjik Kim, Marta Garnelo, David Saxton, Pushmeet Kohli, SM Eslami, and Yee Whye Teh. Meta-learning surrogate models for sequential decision making. *arXiv preprint arXiv:1903.11907*, 2019.
- Marta Garnelo, Dan Rosenbaum, Christopher Maddison, Tiago Ramalho, David Saxton, Murray Shanahan, Yee Whye Teh, Danilo Rezende, and S. M. Ali Eslami. Conditional neural processes. In Jennifer Dy and Andreas Krause, editors, *Proceedings of the 35th International Conference on Machine Learning*, volume 80 of *Proceedings of Machine Learning Research*, pages 1704–1713, Stockholmsmässan, Stockholm Sweden, 10–15 Jul 2018. PMLR. URL <http://proceedings.mlr.press/v80/garnelo18a.html>.
- Greg Brockman, Vicki Cheung, Ludwig Pettersson, Jonas Schneider, John Schulman, Jie Tang, and Wojciech Zaremba. Openai gym, 2016.
- Emanuel Todorov, Tom Erez, and Yuval Tassa. Mujoco: A physics engine for model-based control. In *Intelligent Robots and Systems (IROS), 2012 IEEE/RSJ International Conference on*, pages 5026–5033. IEEE, 2012. URL <https://ieeexplore.ieee.org/abstract/document/6386109/>.
- Edouard Leurent. An environment for autonomous driving decision-making. <https://github.com/eleurent/highway-env>, 2018.
- Stefano V Albrecht and Peter Stone. Autonomous agents modelling other agents: A comprehensive survey and open problems. *Artificial Intelligence*, 258:66–95, 2018.

## Supplementary Material

### S1 Simulation Environments

We present details of the three non-stationary simulation environments in this section. Since we deal with real-world physical tasks, each kind of task has its own dynamics type. The RL agent encounters different types of dynamics sequentially in our setting. The switch of dynamics is assumed to finish within a single timestep. Each type of dynamics may last for several episodes, and we call each episode as one subtask since the dynamics type within an episode is invariant. Note that our method is not restricted by the episodic assumption since the task index and task boundary are unknown. A summary of the key parameters is shown in Table 1.

#### S1.1 Changeable Pole Length and Mass of CartPole-SwingUp

CartPole-SwingUp consists of a cart moving horizontally and a pole with one end attached at the center of the cart. We modify the simulation environment based on the OpenAI Gym environment [Brockman et al., 2016]. Different types of dynamics have different pole mass  $m$  and pole length  $l$ . In our setting, the agent encounters four types of dynamics sequentially with the combinations  $(m, l)$  as  $(0.4, 0.5)$ ,  $(0.4, 0.7)$ ,  $(0.8, 0.5)$ ,  $(0.8, 0.7)$ . Denote the position of the cart as  $x$  and the angle of the pole as  $\theta$ . The state of the environment is  $\mathbf{x} = (x, \dot{x}, \cos \theta, \sin \theta, \dot{\theta})$  and action  $\mathbf{u}$  is the horizontal force applied on the cart. Therefore, the GP input is a 6 dimensional vector  $\tilde{\mathbf{x}} = (\mathbf{x}, \mathbf{u})$ . The GP target is a 5 dimensional vector as the state increment  $\mathbf{y} = \Delta \mathbf{x} = (\Delta x, \Delta \dot{x}, \Delta \cos \theta, \Delta \sin \theta, \Delta \dot{\theta})$ .

#### S1.2 Varying Torso Mass in HalfCheetah

In HalfCheetah, we aim to control a halfcheetah in flat ground and make it run as far as possible. The environment is modified based on MuJoCo [Todorov et al., 2012]. We notice that the torso mass  $m$  significantly affects the running performance. Therefore, we create two different types of dynamics by changing the torso mass  $m$  iteratively between 14 and 34 to simulate real-world delivery situations. We denote the nine joints of a halfcheetah as (root\_x, root\_y, root\_z, back\_thigh, back\_shin, back\_foot, front\_thigh, front\_shin, front\_foot). The state  $\mathbf{x}$  is 18-dimensional consisting of each joint’s position and velocity. The action  $\mathbf{u}$  is 6-dimensional, including the actuator actions applied to the last six physical joints. Therefore, the GP input  $\tilde{\mathbf{x}} = (\mathbf{x}, \mathbf{u})$  is a 24-dimensional, and the GP target is the 18-dimensional state increment  $\mathbf{y} = \Delta \mathbf{x}$ .

#### S1.3 Dynamic Surrounding Vehicles in Highway-Intersection

The Highway-Intersection environment is modified based on highway-env [Leurent, 2018]. We adapt the group modeling [Albrecht and Stone, 2018] concept and treat all the other surrounding vehicles’ behaviors as part of the environment dynamics. In addition to modeling the interactions (analogous to the effect of ego vehicle action to other vehicles), the mixture model also needs to learn the ego vehicles’ dynamics (analogous to the action’s effect on ego vehicle). For simplicity, we only experiment with environments containing only one surrounding vehicle. Note that the multi-vehicle environment can be generated by following the same setting but requires modification of pipelines. For example, to evaluate the posterior probability of all surrounding vehicles from GP components, we can query the mixture model multiple times and then calculate the predictive distribution for each vehicle.

We consider an intersection with a two-lane road. The downside, left, upside, and right entry is denoted with index 0,1,2,3, respectively. The ego vehicle  $A_0$  has a fixed initial state as the right lane of entry 0 and a fixed destination as the right lane of entry 1. In other words,  $A_0$  tries to do a left turn with high velocity and avoid collision with others. Each type of dynamics has different start and goal positions of the surrounding vehicle  $A_1$ .  $A_0$  encounters three types of interactions with the combinations of  $A_1$ ’s start entry and goal entry as  $(2, 1)$ ,  $(2, 0)$  and  $(1, 2)$ . Note that when  $A_1$  emerges at entry 2 and heading to entry 0,  $A_0$  faces a typical unprotected left turn scenario.

Denote the positions and heading of a vehicle as  $(x, y, h)$ . The state of  $A_0$  is  $(x, y, \dot{x}, \dot{y}, \cos h, \sin h)$  in the world-fixed frame. The state of  $A_1$  is  $(x_{rel}, y_{rel}, \dot{x}_{rel}, \dot{y}_{rel}, \cos h_{rel}, \sin h_{rel})$  evaluated in the body frame fixed at  $A_0$ . We directly control the ego vehicle  $A_0$ ’s acceleration  $a$  and steering angle  $\theta$ .

Table S1: Simulation Environment Details. Each type of dynamics last for 3 episodes.

Environment	CartPole	HalfCheetah	Intersection
State Dimension	5	18	12
Action Dimension	1	6	2
Episode Length	200	200	40
Simulation Interval (s)	0.04	0.01	0.1
Early Stop	True when $x$ out of limit	False	True when Collision
No. episodes / Dynamics	3	3	3

Table S2: Model Parameters.

Parameter	CartPole	HalfCheetah	Intersection
concentration parameter $\alpha$	0.1	1.5	0.5
sticky paramter $\beta$	1	1	1
initial noise $\sigma_i, i = 1, \dots, c$	0.001	0.1	0.001
initial output scale $w_i, i = 1, \dots, c$	0.5	10.0	0.5
initial lengthscale $1/w_{i,j}, i, j = 1, \dots, c$	1.0	1.0	1.0
merge KL threshold $\epsilon$	20	10	70
merge trigger $n_{merge}$	15	5	10
data distillation trigger $n_{distill}$	1500	2000	1500
inducing point number $m$	1300	1800	1300
GP update Steps / timestep	10	5	10
learning rate	0.1	0.1	0.1
discount $\gamma$	1	1	1
MPC plan horizon	20	15	20
CEM popsize	200	200	200
CEM No. elites	20	10	20
CEM iterations	5	5	5

Therefore, the GP input  $\tilde{x}$  is a 14 dimensional vector consisting of the  $A_0$ 's state and action as well as  $A_1$ 's state. The GP target is the increment of the ego vehicle's and the other vehicle's states.

## S2 Method Details

The computing infrastructure is a desktop with twelve 64-bit CPU (model: Intel(R) Core(TM) i7-8700K CPU @ 3.70GHz) and a GPU (model: NVIDIA GeForce RTX 2080 Ti). Since our method is pre-train free, we do not need to collect data from different dynamics beforehand. However, for most of the baselines, we collect data to pre-train them as detailed in Section S2.2. In our online setting, there is no clear boundary between training and testing. More concretely, at each time step, our model is updated by the streaming collected data and evaluated in MPC to select the optimal action.

### S2.1 Parameters of Our Method

We list key parameters of our proposed method in Table S2. The concentration parameter  $\alpha$  controls the generation of new GP components. The larger the  $\alpha$ , the more likely a new GP component is spawned. The sticky parameter  $\beta$  increases the self-transition probability of each component. The initial parameter  $\theta_0$  for a new GP consists of initial noise  $\sigma_i$ , initial output scale  $w_i$  and initial lengthscale  $1/w_{i,j}$ . Larger lengthscale and output scale help alleviate the overfitting problem by increasing the effect from the away points. HalfCheetah has a higher state dimension than the other two and thus has larger  $n_{distill}$  and  $m$ . The planning horizon of Intersection is half of the total episode length since the MPC needs to do predictive collision check to achieve safe navigation. For the hyperparameter selection, we randomly search in a coarse range first and then do a grid search in a smaller hyperparameter space.

Table S3: Parameters of the DNN, ANP and MAML Baselines.

Baseline	Parameter	CartPole	HalfCheetah	Intersection
	pre-train episodes / dynamics	10	10	10
DNN	gradient steps	200	100	100
	optimizer	Adam	Adam	Adam
	learning rate	0.0005	0.001	0.008
	hidden layers	2	2	2
	units per layer	256	500	256
	minibatch size	512	256	128
ANP	gradient steps	200	800	100
	optimizer	Adam	Adam	Adam
	learning rate	0.0005	0.001	0.0005
	hidden layers	[256, 128, 64]	[512, 256, 128]	[256, 128, 64]
	minibatch size	1024	64	1024
	context number	100	100	100
	target number	25	25	25
latent dimension	64	128	64	
MAML	hidden layers	2	2	2
	units per layer	500	500	500
	step size $\alpha$	0.01	0.01	0.01
	step size $\beta$	0.001	0.001	0.001
	meta steps	200	100	100
	adapt learning rate	0.001	0.001	0.001
	adapt step	10	10	10
	meta batch size	1	1	1

## S2.2 Parameters of Baselines

The critical parameters of using a DNN, an ANP [Kim et al., 2019, Qin et al., 2019], and a MAML [Finn et al., 2017] are shown in Table S3. The parameters for a single GP baseline and the concentration parameter  $\alpha$  of the DPNN baseline are the same as the corresponding ones of our proposed method, as in Table S2. The DNN parameters in DPNN baseline is the same as the parameters of a single DNN, as in Table S3. Note that except for the baseline using a single GP as dynamics models, all the other baselines require to collect data to pre-train the model. In our setting, we collect ten episodes from each type of dynamics as the pre-train dataset. The parameters for baselines are all carefully selected to achieve decent and equitable performance in our nonstationary setting. For instance, since HalfCheetah has a larger state dimension than the other two, it has larger units per layer in DNN and latent dimension in ANP.

To adapt the MAML method, in addition to the pre-train free assumption, we further release the assumption that the task boundaries between different dynamics are unknown during the pre-train procedure. Note that MAML is pre-trained with the same amount of data as the other baselines to guarantee a fair comparison. The performance of MAML may increase if collecting more data. During the online testing period, the adapt model copies meta-model’s weights and updates its weights with recently collected data at each timestep.

## S3 Additional Experiment Results

### S3.1 Dynamics Assignments with Dirichlet Process Prior

We show that using pure DP prior is not sufficient to capture the dynamics assignments of streaming data in real-world physical tasks by visualizing the cluster results in CartPole-SwingUp, as in Figure 4. In this section, we show more statistics about the dynamics assignments with DP prior by comparing the performance of DPNN and our method in Figure S1.

In CartPole-Swingup, we can see that our method can accurately detect the dynamics shift and cluster the streaming data to the right type of dynamics. However, when using DPNN, the more types of dynamics encountered, the less accurate the assignments are. In Highway-Intersection,

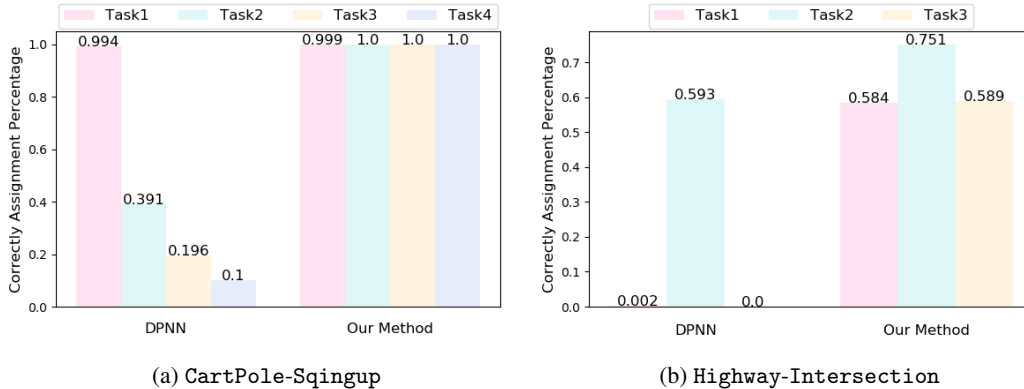


Figure S1: Correct Assignment Percentage using DPNN and our method. Our method outperforms DPNN in terms of task assignments.

Table S4: Reward Mean and Standard Deviation (std). The bold numbers indicate the maximum means and minimum stds in each task.

		CartPole				HalfCheetah		Intersection		
		Task1	Task2	Task3	Task4	Task1	Task2	Task1	Task2	Task3
Our Method	mean	177.62	<b>183.10</b>	<b>181.37</b>	<b>182.54</b>	<b>36.11</b>	<b>34.14</b>	60.66	<b>54.77</b>	<b>52.48</b>
	std	6.61	<b>3.29</b>	<b>1.86</b>	<b>1.10</b>	<b>9.22</b>	13.05	1.29	<b>1.80</b>	<b>0.77</b>
GP	mean	178.04	169.46	174.45	171.67	2.70	-21.26	53.73	39.23	44.25
	std	<b>3.40</b>	7.39	8.94	6.12	14.70	24.49	6.56	20.31	6.91
DNN	mean	176.57	164.72	177.74	164.21	28.89	0.53	43.42	2.31	46.62
	std	8.14	16.41	5.21	7.24	35.02	15.60	9.73	7.34	6.12
ANP	mean	175.33	170.74	171.29	160.87	-4.27	-20.70	<b>62.68</b>	44.04	36.91
	std	6.61	4.44	6.68	8.34	16.80	22.09	<b>0.75</b>	17.95	19.86
MAML	mean	144.91	150.80	127.55	134.36	-70.49	-51.32	39.29	39.14	40.31
	std	28.22	18.74	32.82	13.95	36.57	12.13	3.36	4.21	5.89
DPNN	mean	<b>187.24</b>	182.52	180.20	161.58	-42.88	-39.30	59.97	46.89	18.64
	std	5.03	6.82	3.09	45.27	16.37	<b>8.14</b>	2.92	15.33	22.42

our method sometimes cluster the data points into the wrong dynamics. We hypothesize that this may be due to the overlap in the spatial domain of different interactions. However, our method still outperforms the DPNN in terms of dynamics assignments. DPNN can only stably identify the second task, and either frequently generate new clusters for the first and third task or identify them as the second task. We notice that the clustering accuracy of DPNN heavily relies on the number of previous states concatenated (the length of the short term memory) [Nagabandi et al., 2019]. To make the dynamics assignment of DPNN more stable, in our setting, we use 50 (1/4 episode length) previous data points to determine the dynamics assignment in `CartPole` and 20 (1/2 episode length) in `Intersection`.

### S3.2 Will Dynamics Assignments Affect Task Performance?

To investigate whether the correct dynamics assignments improve the task performance, we compare the accumulated subtask rewards of our method, the single GP baseline, and the DPNN baseline. The single GP baseline is the ablation version of our method without dynamics assignments. In other words, using a single GP indicates clustering different dynamics into a single cluster. The DPNN has less accurate dynamics assignments than our method, as detailed in Section S3.1.

Table S4 and Figure 5 show that our method has higher rewards and smaller variances than the baselines in most situations. Since our method performs better than the single GP baseline in all three nonstationary environments, it shows that the dynamics recognition help increase the task performance. Note that DPNN has higher rewards than our method in the first task of `CartPole-SwingUp`. We hypothesize that this may be due to the pre-train procedure of DPNN. However,



our method outperforms DPNN in all the other dynamics, which indicates that accurate dynamics assignments help improve task performances.

## S4 Model Derivation

In this part, we highlight the derivation of the soft assignment  $\rho_n(z_{nk})$  in 2 that was originally derived in [Tank et al., 2015] Eq.12-16 to ease reading. Note that we highly recommend reading [Tank et al., 2015] for thorough understanding. The posterior distribution  $p_n(z_{0:n}, \boldsymbol{\theta} | \mathcal{D})$  for the assignments  $z_{0:n}$  and model parameter  $\boldsymbol{\theta}$  can be written as product of factors

$$\begin{aligned} p_n(z_{0:n}, \boldsymbol{\theta} | \mathcal{D}) &\propto p((\tilde{\boldsymbol{x}}_n, \boldsymbol{y}_n) | \boldsymbol{\theta}_{z_n}) p(z_n | z_{0:n-1}) p_{n-1}(z_{0:n-1}, \boldsymbol{\theta} | \mathcal{D}_{0:n-1}) \\ &\propto p(\boldsymbol{\theta}) \prod_{i=0}^n p((\tilde{\boldsymbol{x}}_i, \boldsymbol{y}_i) | \boldsymbol{\theta}_{z_i}) p(z_i | z_{1:i-1}) \end{aligned} \quad (\text{S1})$$

Since S1 is in factorized form, we can apply Assumed Density Filtering (ADF) to approximate the posterior of the first 0 to n data pair with  $\hat{q}_n(z_{0:n}, \boldsymbol{\theta}) = \prod_{k=0}^{\infty} \gamma_n(\boldsymbol{\theta}_k) \prod_{i=0}^n \rho_n(z_i)$ . The approximate posterior for the  $n + 1$ -th data pair is thus

$$\hat{p}_{n+1}(z_{0:n+1}, \boldsymbol{\theta} | \mathcal{D}_{0:n+1}) \propto p((\tilde{\boldsymbol{x}}_{n+1}, \boldsymbol{y}_{n+1}) | \boldsymbol{\theta}) p(z_{n+1} | z_{0:n}) \hat{q}_n(z_{0:n}, \boldsymbol{\theta}) \quad (\text{S2})$$

$$\hat{q}_{n+1}(z_{0:n+1}, \boldsymbol{\theta}) = \arg \min_{q_{n+1} \in \mathcal{Q}_{n+1}} KL(\hat{p}_{n+1}(z_{0:n+1}, \boldsymbol{\theta} | \mathcal{D}_{0:n+1}) || q_{n+1}(z_{0:n+1}, \boldsymbol{\theta})) \quad (\text{S3})$$

With the mean field assumption, the optimal distribution for the new observation is given in 2.